Cosmic-ray muon spectrum up to 1 TeV at 75° zenith angle

H. Jokisch, K. Carstensen,* W. D. Dau, H. J. Meyer,† and O. C. Allkofer
Institut für Kernphysik, University of Kiel, Germany
(Received 23 October 1978)

The spectrum of about 6×10^5 muons in the zenith angle range $\theta = 68°$–$82°$ and the energy range $E = 1$–1000 GeV has been measured by a Kiel-Desy collaboration at Hamburg. The data are represented by a simple form fit which goes as $E^{-2.57}\sec\theta$ for the integral spectrum at very high energies. indicating that the galactic cosmic-ray nucleon spectrum is flatter than $E^{-2.75}$ beyond 1000 GeV.

I. INTRODUCTION

The investigation of cosmic-ray muons at sea level provides information about the primary galactic cosmic-ray nucleons in the energy range above 10^{11} eV (where the direct measurements fail) and below 10^{15} eV (the onset of the more indirect extensive-air-shower method). For example, the muon charge ratio is directly coupled to the neutron/proton ratio in galactic cosmic-ray nuclei.[1] The muon spectrum and its zenith-angle dependence at sea level reflects the parent spectra of pions and kaons in the atmosphere[2] and can be related to the primary galactic nucleon spectrum by scaling the interaction properties of hadrons from the accelerator energy range up to higher energies. [All muons above a certain threshold energy E_c are produced by galactic nucleons with a median energy of about 10 E_c (Ref. 3)].

Our high-statistics experiment at large zenith angles complements the recent measurements (of comparable counting rates) at intermediate angles[4] and at vertical direction.[5,6]

II. EXPERIMENTAL

The experimental setup is shown in Fig. 1 and the main properties are listed in Table I.

An air gap magnet was used, so the magnetic field was exactly known and there were no problems with multiple scattering of muons. The spectrometer was triggered by a coincidence of the four scintillation counters, and the muon track was recorded in 14 wire spark chambers which were read out by an on-line computer. Capacitive readout was used for the chambers in the strong stray fields near the magnet, but for the subsequent chambers core and magnetostrictive readout could be applied.

After the careful optical surveying of all spark chambers they were realigned again by iterative fitting of muon tracks; the iterations stopped when the successive corrections were less than 0.1 mm. The final realignment shifts were less than 1 mm, the spatial resolution of 90% of the spark chambers was between 0.53 and 1.0 mm in the bending plane.

In order to avoid errors introduced by possible misalignment and inefficiency (at the edges) of the scintillators, the geometrical acceptance of 360 cm^2 sr was reduced to 274.7 cm^2 sr in offline analysis by the requirement that the calculated track had to penetrate the scintillation counters within the reduced areas and that its zenith angle was in the range 68°–82°. This method was also used for the determination of the efficiency of the two scintillation counters in the magnet gap. The inefficiency correction for the four-fold coincidence was +9.1% and +4.9% for the positive and negative magnetic fields, respectively.

To get a really absolute intensity an additional correction for extensive air showers and noise triggers was performed with the help of a time-of-flight measurement of the muons (with a resolution of $\sigma = 1$ nsec). The correction due to this amounts to -3%. The resulting trigger rate is 9.7/min (Table I).

A more detailed description of the spectrometer and its performance is given in Ref. 7.

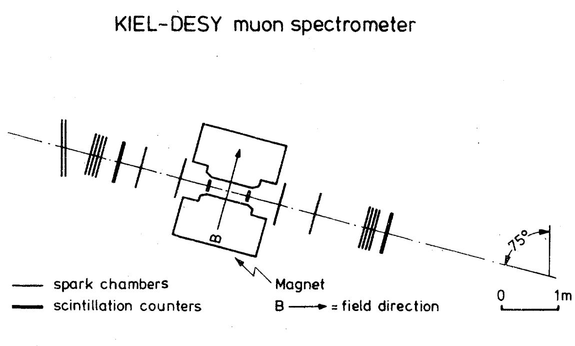

FIG. 1. Experimental setup.

III. DATA ANALYSIS

All the measured events were binned by zenith angles (θ) from 68° to 82° (bin size 2°) and by 30

TABLE I. Main properties of the experimental setup.

magnet:	air gap 27×135 cm^2; deflection power: $\int Bdl = 1.83$ Tm
mdm (mean value):	745 GeV/c
collecting power:	360 cm^2 sr, reduced to 274.7 cm^2 sr
total number of events:	10^6
number of momenta >1 GeV/c:	reduced to 590 958
zenith angle:	$75° \pm 7°$
azimuth:	$288° \pm 20°$ (east)
detectors:	4 scintillation counters 14 wire spark chambers
rate (corrected):	9.7 min^{-1} ± 5% (95% confidence)

momentum (p) intervals. For each of the seven zenith-angle intervals model spectra (four parameters) were fitted to the frequencies of the 30 momentum bins after folding in the acceptance and resolution functions. [The acceptance function $A(p,\theta)$ depends on the geometry of the spectrometer and is constant beyond 10 GeV/c and decreases to zero below 1 GeV/c. The resolution function $F(\psi-\psi_p)$ gives the probability that a deflection angle ψ is measured when an angle $\psi_p = 1/p$ is expected. The resolution function used here was the *experimental* deflection error distribution which was calculated from the errors of the parameters of each individual event-track fit. As the number of sparks determining a track varies because of inefficiencies between 4 and 14 (most probable number =12) the error distribution $F(\psi-\psi_p)$ is not a Gaussian with a fixed standard error σ_ψ. So the commonly used term "maximum detectable momentum" (mdm) (which is defined by $\text{mdm}\times\sigma_\psi = p\times\psi$) does not give an exact description of a spectrometer. Our mdm values range from 250 to 1200 GeV/c, so a "mean mdm" is given in Table I.] The χ^2 values for the spectra fits are in the range 19 to 30 for 26 degrees of freedom.

The ratios of expected frequencies to acceptance- and resolution-corrected frequencies give the final correction factors $R(p,\theta)$ by which the measured frequencies per momentum and angle bin have to be multiplied. Figure 2 shows the function $R(p)$, which is $R(p,\theta)$ averaged over θ, or, more precisely, the factor by which the measured numbers in Table II have to be multiplied to get the correct ones.

IV. RESULTS

To present the final corrected data in a simple way, we fitted the seven differential and seven integral histograms by phenomenological form spectra $D(p,\theta)$ and $I(p,\theta)$, respectively.[8] $D(p,\theta)$ is given by

$$D(p,\theta) = \frac{451_a}{p/\sec\theta + 77.2_b}(5p + 9.2_c \sec\theta)^{-2.57} \times \frac{p+19.8_d}{p+19.8_d\sec\theta}, \quad (1)$$

[where p is in GeV/c and $D(p,\theta)$ is in cm^{-2}sr^{-1}sec^{-1} (GeV/c)$^{-1}$]. The values with indices are the fitted parameters $a = 451\pm15$, $b = 77.2\pm4.8$, $c = 9.2\pm0.5$, $d = 19.8\pm1.8$ (degrees of freedom DF =94, $\chi^2 = 1.21 \times \text{DF}$). $I(p,\theta)$ is given by

$$I(p,\theta) = \frac{35_r}{p/\sec\theta + 57.3_s}(5p + 11.4_t \sec\theta)^{-1.57} \times \frac{p+8.9_u\times 3}{p+8.9_u(2+\sec\theta)}, \quad (2)$$

where $I(p,\theta)$ is in cm^{-2} sr^{-1} sec^{-1}, $r = 35.0\pm1.1$,

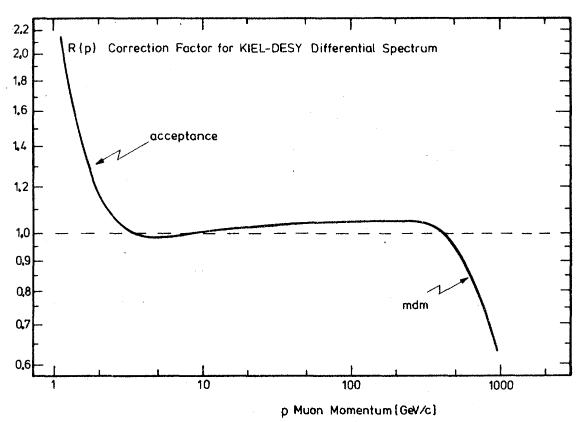

FIG. 2. The correction factor $R(p)$. $R(p)$ has to be applied to the measured differential spectrum. The regions of large influence by the geometric acceptance and by the finite resolution (mdm effect) of the spectrometer are indicated by arrows.

TABLE II. Differential intensities.

Momentum p (GeV/c)	Intensity $[\mathrm{cm}^{-1}\,\mathrm{sr}^{-1}\,\mathrm{sec}^{-1}(\mathrm{GeV}/c)^{-1}]$	Error (%)	Measured number
1.12	2.973×10^{-5}	1.45	4 782
1.41	3.111×10^{-5}	1.07	8 751
1.76	3.263×10^{-5}	0.85	13 876
2.29	3.168×10^{-5}	0.71	19 604
2.85	3.068×10^{-5}	0.63	25 368
3.57	2.848×10^{-5}	0.57	30 900
4.49	2.606×10^{-5}	0.53	36 244
5.66	2.332×10^{-5}	0.49	40 920
7.12	2.021×10^{-5}	0.48	44 192
8.95	1.705×10^{-5}	0.46	46 468
11.26	1.373×10^{-5}	0.46	46 910
14.17	1.070×10^{-5}	0.47	45 497
17.83	8.029×10^{-6}	0.48	42 596
22.44	5.708×10^{-6}	0.51	37 938
28.23	3.964×10^{-6}	0.55	33 075
35.52	2.637×10^{-6}	0.60	27 560
44.70	1.712×10^{-6}	0.67	22 421
56.25	1.064×10^{-6}	0.76	17 488
70.79	6.479×10^{-7}	0.86	13 465
89.09	3.751×10^{-7}	1.01	9 771
112.13	2.208×10^{-7}	1.18	7 241
141.12	1.234×10^{-7}	1.41	5 027
177.62	6.632×10^{-8}	1.70	3 440
223.56	3.735×10^{-8}	2.06	2 408
281.39	1.869×10^{-8}	2.53	1 559
354.18	9.689×10^{-9}	3.15	1 008
445.81	5.436×10^{-9}	3.92	759
625.46	1.770×10^{-9}	3.87	793
990.22	3.982×10^{-10}	6.30	370

$s=57.3\pm2.9$, $t=11.4\pm0.4$, $u=8.9\pm0.8$, DF=101, $\chi^2=1.22\times\mathrm{DF}$.

The differential spectrum $D(p,\theta)$ is not the derivative dI/dp of the integral spectrum $I(p,\theta)$, but the expression D is much simpler than dI/dp and gives the same good fit results.

The fits were restricted to momenta beyond 30 GeV/c where geomagnetic deflection and multiple scattering of the muons in the atmosphere are completely negligible. The three terms in $D(p,\theta)$ and $I(p,\theta)$ correspond to pion decay (proportional to $\sec\theta/p$), pion production spectrum (proportional to $p^{-\gamma}$) and muon decay with energy loss (3rd term), respectively. The pion production spectrum's exponent γ was not taken as a fit parameter, because it has already been shown[9] that $\gamma=2.57\pm0.03$ gives the best fit to our data as well as to both other high statistics experiments at smaller zenith angles.[4-6]

The relative deviations of the measured spectra to the corresponding form fit at zenith angle θ were averaged over θ and shown in Figs. 3 (differential) and 4 (integral) as black dots. The maximum deviations which occur for the extreme zenith angle bins are also given.

Our form fit represents remarkably well even

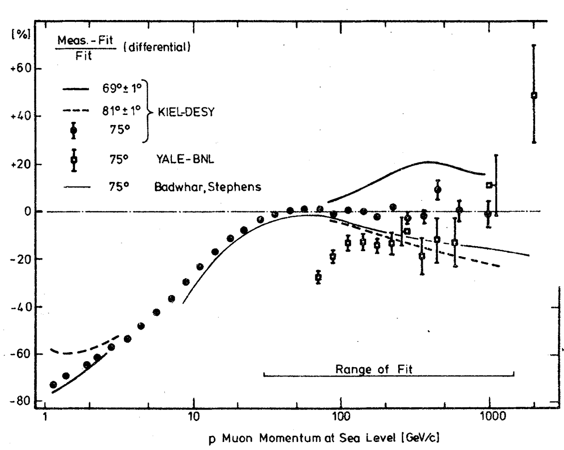

FIG. 3. The relative differences of measured (or calculated) differential spectra to the form fit at 75° zenith angle.

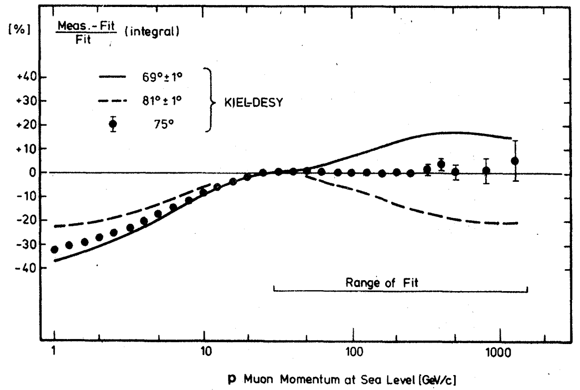

FIG. 4. The relative differences of measured integral spectra to the form fit at 75° zenith angle.

the vertical data of the Durham Spectrometer,[5] which would show up in Fig. 3 on the 69° curve (>30 GeV/c). The Yale-BNL data[10] for $\theta = 75°$ are also given for comparison in Fig. 3.

Our actual measured intensities are presented in Tables II (differential) and III (integral). They refer to $\theta = 75°$ but include all data from 68° to 82°. This was possible by modulating the 75° form fit with the average deviation curves from Figs. 3 and 4. The errors are standard errors of the counting rates. The error of the absolute calibration is given in Table I (rate). To visualize the steepness of the muon spectrum, the integral data (Table III) are shown in Fig. 5 together with the form fit and a pure power-law spectrum.

TABLE III. Integral intensities.

Momentum p (GeV/c)	Intensity ($cm^{-2}\,sr^{-1}\,sec^{-1}$)	Error (%)	Measured number
1.00	4.743×10^{-4}	0.13	590 958
1.26	4.664×10^{-4}	0.13	586 176
1.58	4.560×10^{-4}	0.13	577 425
2.00	4.424×10^{-4}	0.13	563 549
2.51	4.253×10^{-4}	0.14	543 945
3.16	4.046×10^{-4}	0.14	518 577
3.98	3.802×10^{-4}	0.14	487 677
5.01	3.523×10^{-4}	0.15	451 433
6.31	3.208×10^{-4}	0.16	410 513
7.94	2.867×10^{-4}	0.17	366 321
10.00	2.507×10^{-4}	0.18	319 853
12.59	2.143×10^{-4}	0.19	272 943
15.85	1.787×10^{-4}	0.21	227 446
19.95	1.452×10^{-4}	0.23	184 850
25.12	1.154×10^{-4}	0.26	146 912
31.62	8.935×10^{-5}	0.30	113 837
39.81	6.761×10^{-5}	0.34	86 277
50.12	4.990×10^{-5}	0.40	63 856
63.10	3.607×10^{-5}	0.47	46 368
79.43	2.548×10^{-5}	0.56	32 903
100.00	1.775×10^{-5}	0.67	23 132
125.89	1.204×10^{-5}	0.81	15 891
158.49	8.018×10^{-6}	1.00	10 864
199.53	5.300×10^{-6}	1.23	7 424
251.19	3.376×10^{-6}	1.53	5 016
316.23	2.159×10^{-6}	1.92	3 457
398.11	1.366×10^{-6}	2.42	2 449
501.19	8.046×10^{-7}	3.08	1 690
794.33	2.863×10^{-7}	5.06	897
1258.92	1.012×10^{-7}	8.48	527

V. DISCUSSION

The Yale-BNL data (Fig. 2), although of poorer statistics, are in good agreement with our data concerning the shape of the spectrum between 100 and 600 GeV/c. Their high-energy points may not be well corrected for the resolution (mdm effect). As they use a hardware momentum selection at 100 GeV/c, their two lowest points should not be given too much weight. Remembering the small error of our absolute rate, there remains a systematic deficit of about 12% for the Yale-BNL data.

In Fig. 2 is also shown the most recent theo-

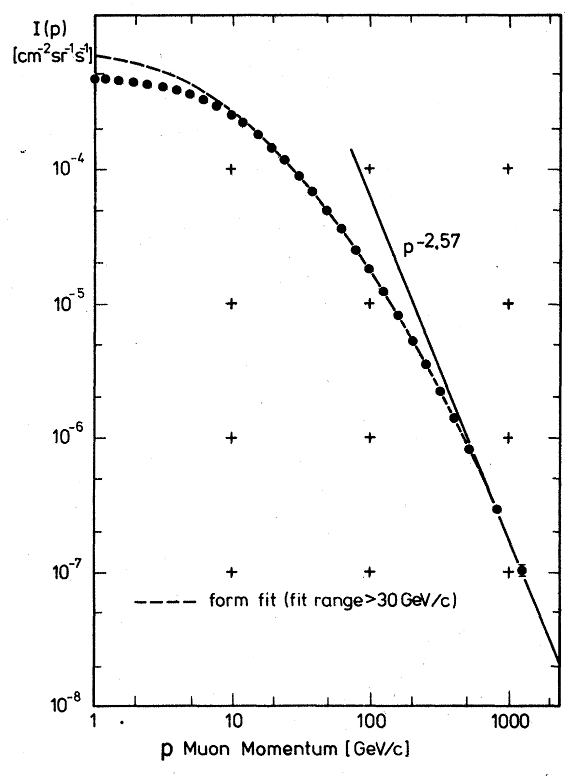

FIG. 5. The integral muon spectrum at 75°. The dashed curve represents the form fit; the straight line shows the asymptotic behavior of the spectrum.

retical calculation of muon spectra which was done especially for 75° zenith angle.[11] The calculation started with the primary galactic nucleon spectrum and solved the pion and kaon transport equation rigorously. The theoretical curve represents remarkably well our data from 10 to 100 GeV/c, but seems to fade out at higher energies. The same effect is seen by comparing the vertical spectrum, calculated in the same way,[12] to measured vertical spectra, as shown by the Kiel group.[9] As Badhwar and Stephens use the spectral index -2.75 for their primary nucleon spectrum (an extrapolation from direct measurements at lower energies) one can conclude that the galactic nucleon spectrum becomes flatter at primary energies beyond 1 TeV.

ACKNOWLEDGMENT

This work was part of the experiment P108 performed at DESY (Deutsches Elektronen Synchrotron), Hamburg. We like to thank our colleagues A. Bäcker, C. Grupen, and W. Stamm for their kind collaboration during our common experiment. It is also a pleasure to acknowledge the technical assistance of the DESY groups F51 and S2. We thank the DESY administration as well as the Deutsche Forschungsgemeinschaft for financial support.

---

*Now at Abteilung Medizinische Statistik und Dokumentation, University of Kiel, Germany.

†Now at Fachbereich Physik, Gesamthochschule Siegen, Germany.

[1] O. C. Allkofer, K. Carstensen, W. D. Dau, and H. Jokisch, Phys. Rev. Lett. 41, 832 (1978).

[2] W. D. Dau, K. Carstensen, and H. Jokisch, in *Proceedings of the Fourteenth International Conference on Cosmic Rays, Munich*, 1975, edited by Klaus Pinkau (Max-Planck-Institute, München, 1975), Vol. 6, p. 1931.

[3] T. K. Gaisser, J. Geophys. Res. 79, 2281 (1974).

[4] T. H. Burnett, G. E. Masek, T. Maung, E. S. Miller, H. Ruderman, and W. Vernon, in *Proceedings of the Thirteenth International Conference on Cosmic Rays, Denver*, 1973 (Colorado Associated Univ. Press, Boulder, 1973), Vol. 3, p. 1764.

[5] C. A. Ayre, J. M. Baxendale, C. J. Hume, B. C. Nandi, M. G. Thompson, and M. R. Whalley, J. Phys. G 1, 584 (1975).

[6] M. G. Thompson, R. Thornley, M. R. Whalley, and A. W. Wolfendale, in *Proceedings of the 15th International Conference on Cosmic Rays, Plovdiv*, 1977, edited by Christo Christov (Institute for Nuclear Research, Sofia, 1977), Vol. 6, p. 21.

[7] K. Carstensen, Ph.D. thesis, University of Kiel, 1978 (unpublished).

[8] S. Miyake, in *Proceedings of the Thirteenth International Conference on Cosmic Rays, Denver*, 1973 (Colorado Associated Univ. Press, Boulder, 1973), Vol. 5, p. 3658.

[9] O. C. Allkofer, K. Carstensen, W. D. Dau, H. Jokisch, and H. J. Meyer, in *Proceedings of the 15th International Conference on Cosmic Rays, Plovdiv*, 1977 edited by Christo Christov (Institute for Nuclear Research, Sofia, 1977), Vol. 6, p. 38.

[10] L. Leipuner, R. Larsen, L. Smith, R. Adair, B. Higgs, H. Kasha, and R. Kellog, in *Proceedings of the Thirteenth International Conference on Cosmic Rays, Denver, 1973* (Colorado Associated Univ. Press, Boulder, 1973), Vol. 3, p. 1771.

[11] G. D. Badhwar and S. A. Stephens, in *Proceedings of the 15th International Conference on Cosmic Rays, Plovdiv*, 1977, edited by Christo Christov (Institute for Nuclear Research, Sofia, 1977), Vol. 6, p. 200, and private communication, 1978.

[12] G. D. Badhwar, S. A. Stephens, and R. L. Golden, Phys. Rev. D 15, 820 (1977).